Pullout Mechanism of Geogrids Under Confinement by Sandy and Clayey Soils

DAVE TA-TEH CHANG, TSUNG-SHENG SUN, AND FAN-YI HUNG

The frictional mechanism of geogrid-soil interaction is considered in two parts: one is passive resistance from the soil mass ahead of the transverse ribs and the other is produced by the frictional resistance. The factors influencing the mechanical performance of geogrid-soil interaction are studied. With three types of geogrids, three types of soils (two sandy soils and one clayey soil), and various testing conditions, a series of pullout tests for geogrid was conducted. Through the testing program, the significance of influencing factors and the strain contribution measured by strain gauges are studied. According to the results of the experiments, the pullout resistance of geogrid tends to increase as the confining pressure is increased. For sandy soils, the passive earth pressure offers the most pullout resistance; when using fine grained soil, it is replaced by friction resistance.

The concept of earth reinforcement involves placing certain materials in the soil to increase the bearing capacity of the soil mass and to stabilize slopes. From the civil engineering standpoint, excessive deformation of the reinforced soil mass is prevented by frictional resistance that occurs where the soil grains are in contact with the reinforcement element.

Geogrid is effective as a reinforcement element because it offers the following two forms of resistance to the pullout failure mechanism when used as a reinforcement element for soil structures: (a) friction between soil and the surface of the geogrid and (b) the passive earth resistance of the soil against the transverse ribs. The researchers' investigations have been focused on ascertaining which of these two offers the greater resistance in the geogrid-soil interaction.

To obtain rational parameters for design, it was taken into consideration that soil available on the work site is generally the backfill material of choice, owing to the difficulty of obtaining sand for use in public construction projects. For this reason a reinforced earth wall demonstration site was established for this study in Tianliao, a mudstone district in Kaohsiung County on the route of a new freeway system. Two types of geogrid were used to examine and compare pullout interaction behavior with sandy and clayey soils.

MECHANISMS OF INTERACTION BETWEEN REINFORCEMENT AND SOIL

Stress transfer between the geogrid and the soil is primarily a function of frictional resistance and passive earth pressure. The former is generated by friction between the soil and the surface of the geogrid; the latter is a function of the grid-shaped construction, which causes the transverse ribs to interlock tightly with the intervening soil. Because pullout force causes the geogrid to move relative to the surrounding soil, passive earth pressure develops against the transverse ribs. Thus a reinforcing effect is attained by bringing into play the latent interaction potential inherent in friction resistance and soil passive resistance.

For pullout-resistance behavior, many properties of soil and geogrid are known as the influence factors (*1*). The pullout resistance to geogrid is thought to be developed by the following two stress-transfer mechanisms: (a) frictional resistance between soil grains and contact grid surface and (b) the resistance from the soil passive mass against the transverse ribs (*2*). To evaluate the frictional resistance (P_f), and ideal expression has been derived and suggested (*3*):

$$P_f = 2A_r\alpha_s \cdot \sigma_v \cdot \tan \delta \quad (1)$$

where

A_r = gross area of geogrid,
α_s = fraction of solid surface area in grid,
σ_v = vertical effective stress, and
δ = friction angle between soil and geogrid surface.

Equation 1, the formula for estimating P_f, is widely accepted and frequently used. The passive resistance of soil bearing on the transverse ribs is a problem similar in kind to the base pressure on deep foundations in soil. Passive resistance is a function of the grid-shaped structure, which causes the transverse ribs to bind tightly with the intervening soil. Because pullout forces cause the geogrid to move relative to the surrounding soil, passive earth pressure develops against the transverse ribs. It has been suggested that this passive earth pressure be expressed in terms of the bearing capacity from the punching failure mode as given in Figure 1 (*2*).

To determine the potential interaction of the geogrid with not only granular soil but also fine-grained soils, a testing device was designed and built for this study. The device was used to ascertain the basic mechanical characteristics of the geogrid during pullout testing under confined conditions. Strain distribution along the geogrid was measured only to supply supplementary data; it is not a focus of this study. The confining box suggested by the Geosynthetic Research Institute (*4*) was not used in this study.

LABORATORY TEST PROGRAM

Materials

Two types of sandy soil were used in the test program: one was collected from the backfill sand used for the test wall in Tianliao,

Civil Engineering Department, Chung Yuan University, Chung Li, Taiwan 32023, R.O.C.

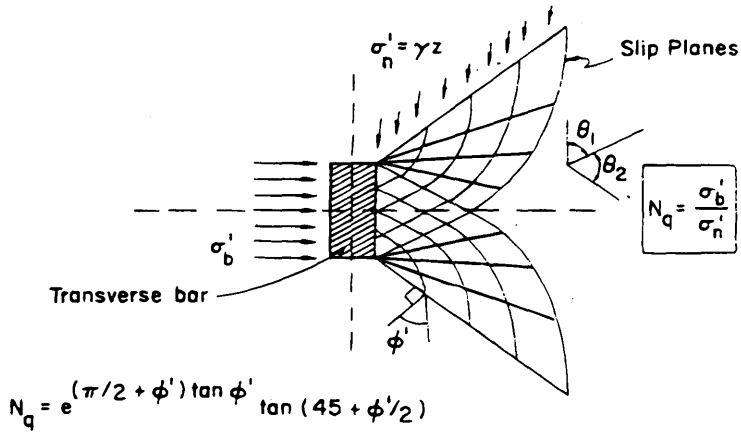

FIGURE 1 Passive bearing punching shear failure mechanism (*2*).

Kaohsiung County, and the other was Ottawa sand (C-190). Relative density for both was controlled at 80 percent. The clayey soil was weathered mudstone, which was also obtained from the same test site in Kaohsiung County. Water content was maintained at OMC + 2 percent, and the degree of compaction was 95 percent. See Table 1 and Figure 2 for the basic properties and grain-size distribution curves of the aforementioned soils. The two types of geogrids used were manufactured from HDPE, labeled "A" and "B" (Table 2). To reduce the boundary effect, samples of the A and B geogrids measuring eight squares in width and three squares in length were used. The portion of each geogrid buried in the soil was fixed at 39 cm. Another part of the study focused on exploring the frictional resistance of the geogrid-soil interface for specimens of the same size. Pullout tests were conducted on the A and B grids from which the transverse ribs had been cut. It is believed that pullout resistance from the trimmed specimen is a factor of frictional resistance only. In addition, the differences in contact area between trimmed specimens and intact specimens must be allowed for so that the frictional resistance for intact grid specimens can be calculated. The passive resistance from the transverse ribs, therefore, is determined for comparison purposes.

Pullout Box

The top and bottom pullout boxes are 40 cm long, 50 cm wide, and 15 cm deep internally, with a 1-cm opening between the two adjacent boxes. See the structural sketch in Figure 3. To prevent boundary effects from occurring, the upper and lower boxes were fitted with sleeves. Below the boxes is an adjustable bearing plate that allows the pulling forces to be aligned into the same plane as the geogrid, pulling it out via the opening between the two boxes. Normal stress is applied using air bags into which compressed air can be directly pumped. Polystyrene packers are placed inside the air bag in the lower box to ensure both that the air compartment in the lower box is completely sealed during compaction of the sample, and that the normal stress is evenly distributed, reducing the effect of the laboratory boundary effect. Normal stress of 0.5, 1.0, and 1.5 kg/cm^2 is applied during the test. The pulling system consists of a constant rate motor assembly. The pulling force can be adjusted through a set of gears.

Measuring System

Two linear variable differential transformers (LVDTs) with a maximum stroke of ± 10 cm are attached to the puller. An amplifier accurate to 10^{-3} mm measures the pullout displacement of the geogrid, and the two LVDTs provide verification. The strain gauges are smeared with paraffin to prevent moisture-induced short circuits, and are cemented to the surface of the rib. In this way, one can ascertain the way strain is distributed when the geogrid is subject to pulling forces. The Kyowa KLM-6-A9 strain gauge with Kyowa EC-30 cement was used; with this combination, strains of up to 20 percent can be measured. The strain gauge is attached to three transverse ribs 2 cm from their junctions, ensuring that the transverse ribs are all the same width at the point of attachment. They are located 5, 21, and 37 cm from the front wall of the box. A Tokyo Sokki Kenkyujo TDS-301 data logger with an amplifier simultaneously records the values registered by load cells, LVDTs, and strain gauges.

Testing Procedures

During testing, strain rate was controlled at 1 mm/min (*4*); the portion of the grid buried in the soil was fixed at 39 cm. The soil in the

TABLE 1 Properties of Tested Soils

Property	Backfill sand	C-190 sand	Weathered mudstone
Dry unit weight, γ_d (g/cm^3)	1.791	1.715	1.865
Angle of internal friction, ϕ	45°	37°	29°
Cohesion, (kg/cm^2)	------	------	0.364

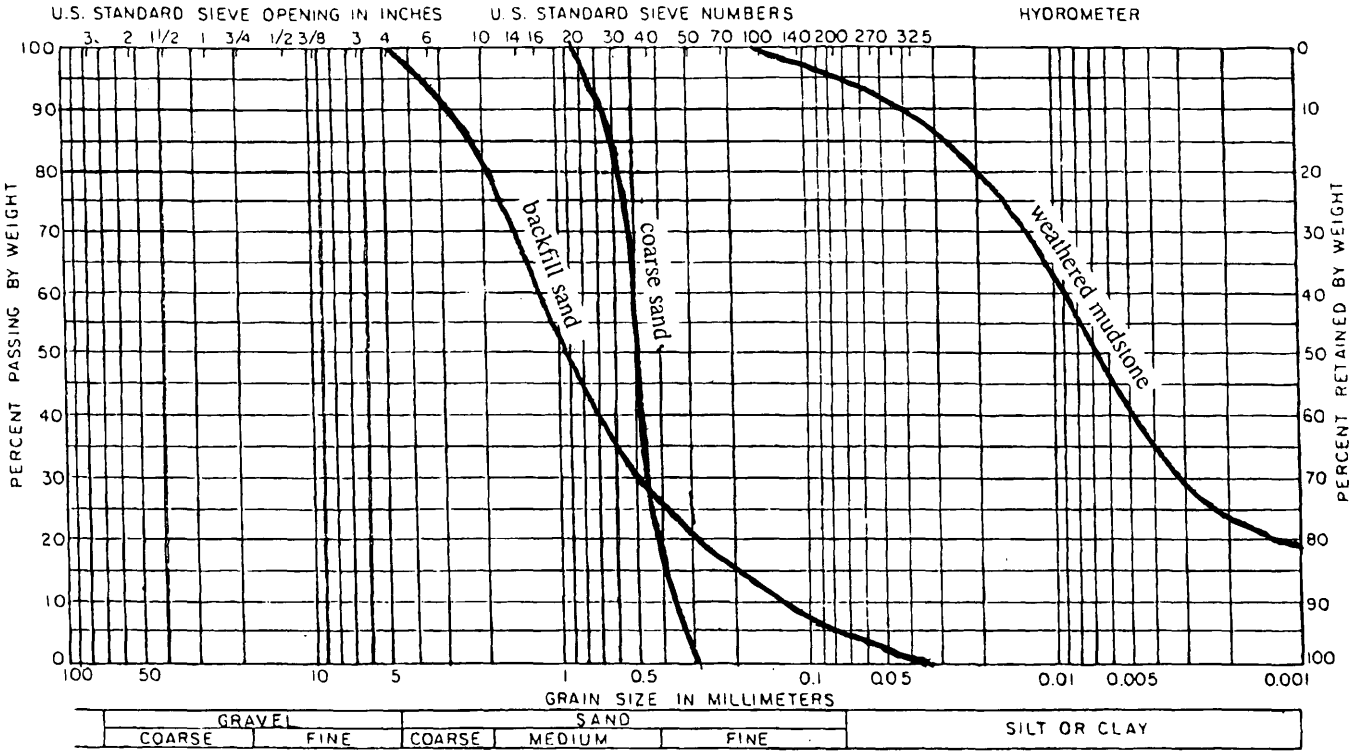

FIGURE 2 Grain size distribution of tested soils.

top and bottom pullout boxes was compacted into the boxes in five even layers, and the geogrid specimen was buried in the middle, aligned with the opening between the boxes and with the direction of pulling-force application. Compressed air was then pumped into the air bags in accordance with the required normal stresses and left for 24 hr so the pressure could equilibrate. The leads from the strain gauges were connected to the data logger, and when the reading from the strain gauge stabilized after 24 hr of pressurization—indicating that settlement of the sample had ceased—the LVDT was placed in position, the motor and data logger were turned on, and the data logger was set to take readings every 10 sec until the pullout forces decreased.

TABLE 2 Properties of Geogrids Used

Geogrid	A	B
Polymer type	HDPE	HDPE
Shape of apertures	oblong	oblong
Thickness of longitudinal ribs, mm	1.4	0.95
Length of longitudinal ribs, mm	144	144
Spacing of longitudinal ribs, mm	16	16
Width of transverse ribs, mm	16	16
Thickness of transverse ribs, mm	3.9	2.7
Thickness of junction, mm	3.9	2.7
Tensile strength, kN/m	87	60
Elongation, %	10.8	8.8

ANALYSIS AND DISCUSSION

As previously discussed, the two main mechanisms of pullout resistance for geogrids are the frictional resistance and the resistance due to passive earth pressure. However the pullout resistance exhibited by the geogrid varies with different soil media.

Effect of Soil Properties on Pullout Behavior of Geogrid

As Figures 4, 5, and 6 show, the geogrid's pullout resistance during initial pullout displacement in backfill sand is actually lower than in coarse sand or weathered mudstone. After completion of initial pullout displacement, pullout resistance rises steadily. This discrepancy arises because backfill sand is well graded and has a high proportion of large grains, which may slide easily when pressed by the transverse ribs. These large grains move until they are packed tightly against the smaller grains, giving rise to greater soil passive resistance and a concurrent steady increase in pullout resistance. The grains in C-190 sand and weathered mudstone have relatively lower ϕ values, so pullout resistance is more likely to stabilize at a constant value when the transverse ribs have caused the soil grains to slide.

To discover the relationship during the experiment between the friction resistance at the surface of the grid and the passive resistance against its transverse ribs, the pullout tests were conducted on A and B grids from which the transverse ribs had been removed. By adjusting the effective contact area of the geogrids in this way and ascertaining their frictional resistance with the soil, a comparison could be made between the frictional resistance figures of geogrids with and without transverse ribs. As shown in Figures 7 and 8, friction resistance makes up 30 percent of the total pullout resistance

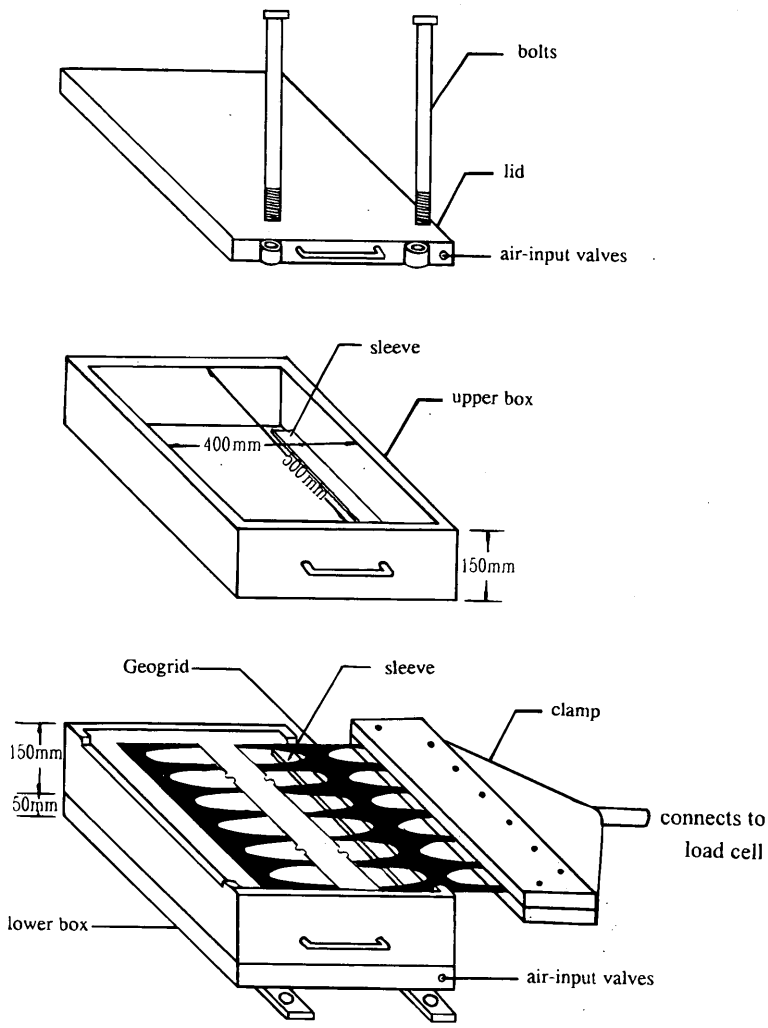

FIGURE 3 Confining pullout box.

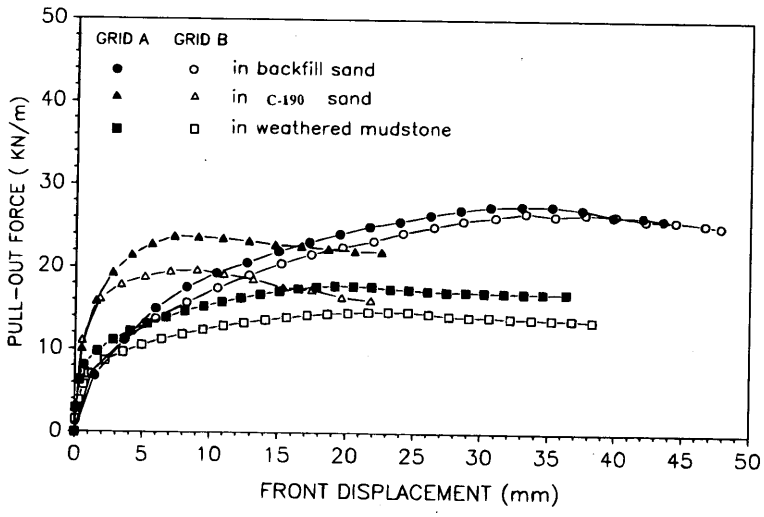

FIGURE 4 Pullout resistance of geogrid under confinement by various soil types at 0.5 kg/cm².

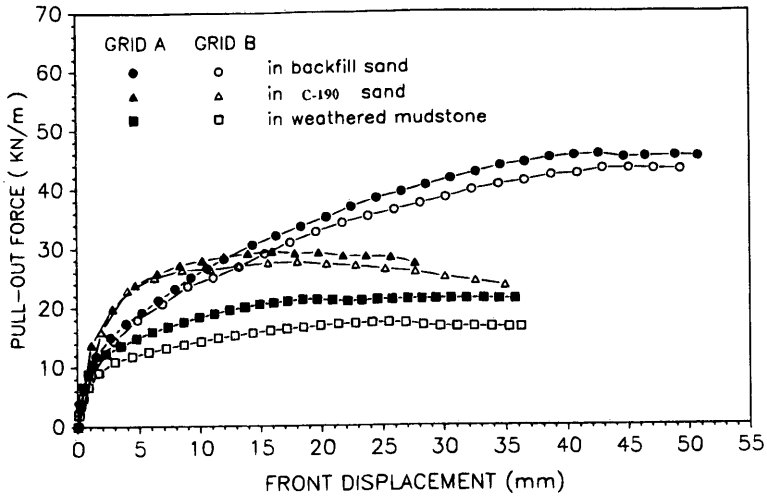

FIGURE 5 Pullout resistance of geogrid under confinement by various soil types at 1.0 kg/cm².

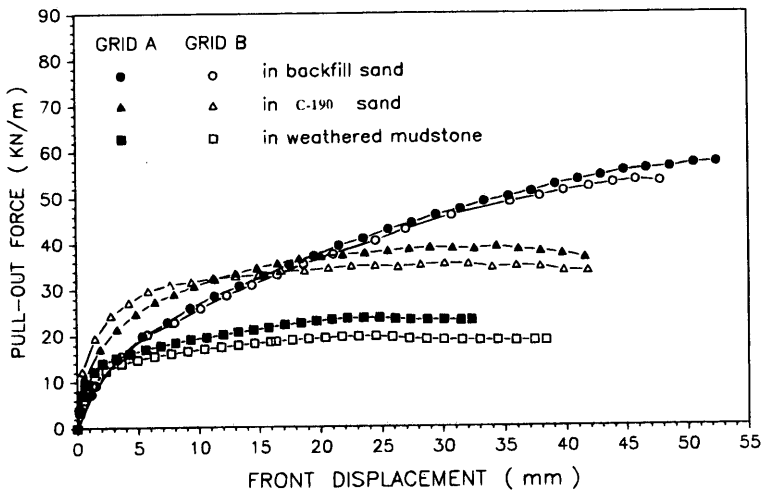

FIGURE 6 Pullout resistance of geogrid under various soil types at 1.5 kg/cm².

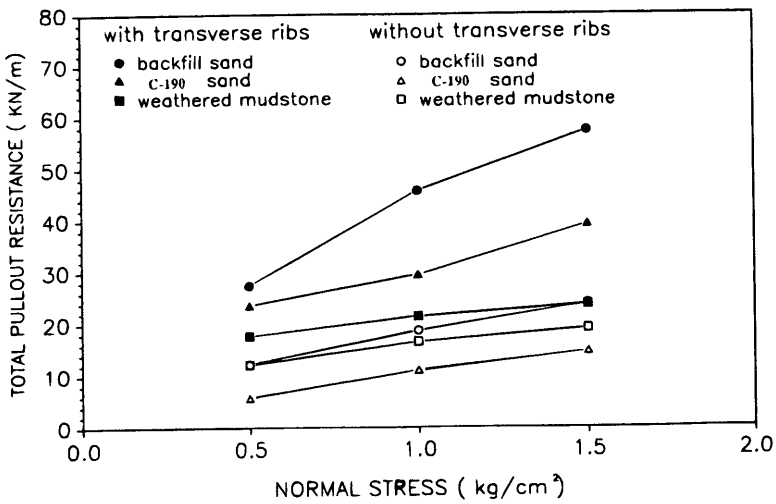

FIGURE 7 Comparison of pullout resistance in A geogrids with and without transverse ribs.

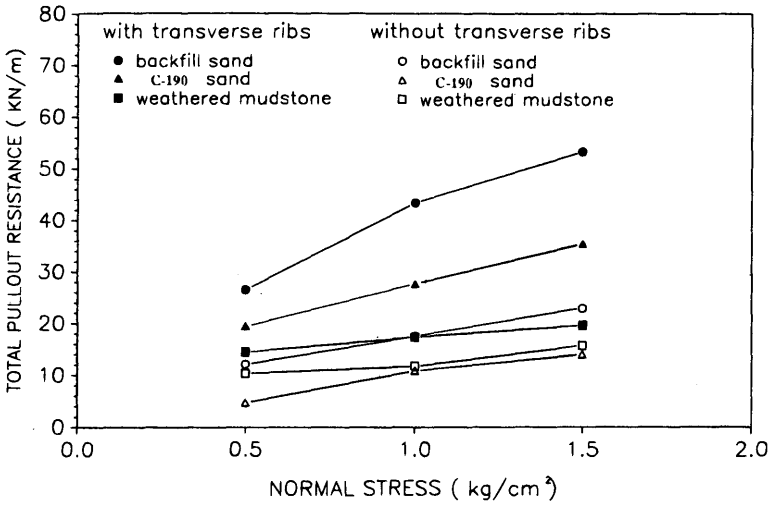

FIGURE 8 Comparison of pullout resistance in B geogrids with and without transverse ribs.

exhibited by the geogrid in sandy soil. The remaining 70 percent is contributed by soil passive resistance; thus, the effect of soil passive resistance is greater than that of frictional resistance. Numerical methods (*5*) were used to predict the components of pullout in dense sand: it was found that passive resistance made up most of the resistance. It can also be seen from Figure 9 that Grid A offers greater pullout resistance than Grid B. Although Grids A and B are almost identical in shape, the transverse ribs of Grid A are 1.2 mm thicker than those of Grid B, so the bearing surface for the soil passive resistance of Grid A is greater than that of Grid B; thus, the bearing surface of the transverse ribs directly influences the amount of soil passive resistance that is developed.

Some interesting findings were discovered in the weathered mudstone test results. A representative confinement finding of 1.5 kg/cm^2 is included in Figure 10. From Figure 10, it is observed that most of the pullout resistance exhibited by the geogrid in clayey soils is contributed by frictional resistance; thus, the frictional resistance effect contributes more to the pullout resistance of the geogrid in weathered mudstone than does soil passive resistance. The findings also indicate that, during the initial stage when pullout displacement had not yet exceeded 2 mm, the total pullout resistance was equivalent to its friction resistance. It was only after this initial stage that total pullout resistance values gradually exceeded the frictional resistance figures. This phenomenon arises in the initial stages, where the displacement that occurs is due to elongation in the front portion of the grid specimen itself, not to relative displacement between the grid and the soil mass. The main resistance to pulling forces is contributed by static friction between the grid and the soil. The soil passive resistance of the transverse ribs develops only when there is relative displacement between the soil and the grid, so it is only when this displacement occurs that total pullout resistance gradually becomes higher than friction resistance.

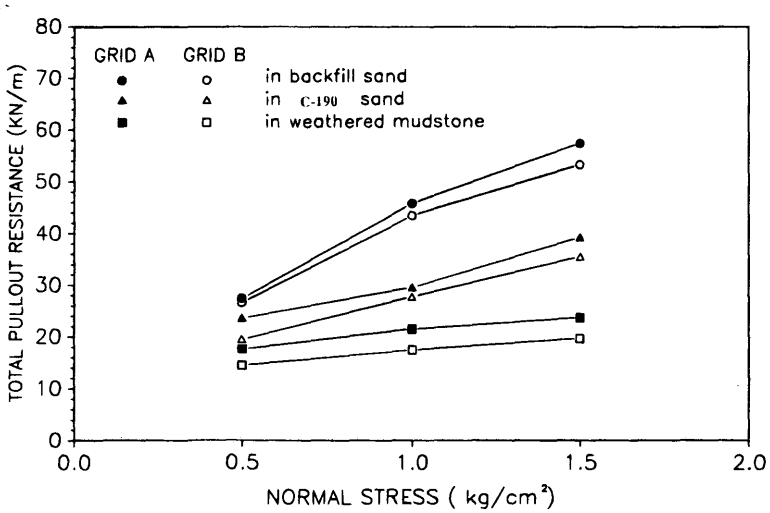

FIGURE 9 Total pullout resistance between geogrid and soil under various confinements.

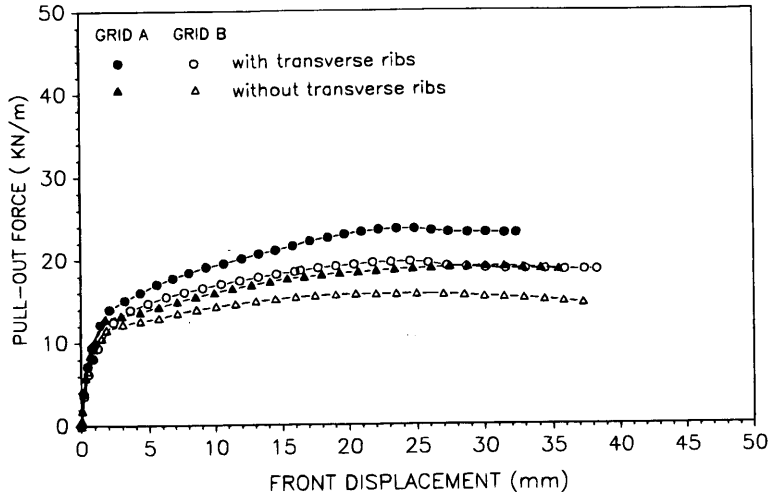

FIGURE 10 Pullout resistance relationships for geogrid under confining pressure of 1.5 kg/cm² in weathered mudstone.

From the evaluation described, it can be summed up that in sandy soils most of the pullout resistance is contributed by soil passive resistance. In clayey soils, frictional resistance provides the largest part of pullout resistance.

Bearing Resistance on Transverse Ribs

As has been pointed out, the pullout resistance is composed of frictional and passive resistance. This can be expressed with the following formula:

$$P_T = P_F + P_B \tag{2}$$

$$P_F = P_{f(LR)} + P_{f(TR)} \tag{3}$$

where

P_T = total pullout force,
P_F = total friction resistance at grid surface during pullout,
P_B = bearing force at transverse ribs,
$P_{f(LR)}$ = surface friction force at longitudinal ribs, and
$P_{f(TR)}$ = surface friction force at transverse ribs.

To calculate the bearing resistance generated at the transverse ribs in this experiment, the transverse ribs were cut from one of two identical geogrid specimens; then pullout tests were conducted for both. Because the resistance figures obtained were a function of the frictional resistance generated at the longitudinal ribs and the cut surface, the following modified formula must be used to obtain true total frictional resistance values during pullout:

$$P_F = \frac{A_{(TR + LR)}}{A_{(LR + \text{cut surface})}} P_{f(LR + \text{cut surface})} \tag{4}$$

where

$P_{f(LR + \text{cut surface})}$ = frictional resistance of longitudinal ribs and the cut surface,
$A_{(TR + LR)}$ = surface area of longitudinal and transverse ribs, and
$A_{(LR + \text{cut surface})}$ = surface area of longitudinal ribs and cut surface.

During pullout in sandy soils, the soil grains at the bearing surface of the transverse ribs are packed into a denser state, thus maximizing the interlocking effect between the soil and the transverse ribs and increasing the passive resistance at the bearing surface. On comparing the bearing forces at the transverse ribs under the effects of different confinements as depicted in Figure 11, it is evident that in backfill sand or coarse sand the bearing force rises as confining pressure is increased. This may be attributed to the densely packed structure of the grains in this well-graded backfill sand, which causes the rate of increase in bearing force to rise as more confining pressure is applied. The bearing force shows no marked increase in uniformly graded coarse sand however. The foregoing phenomenon explains why the angle of internal friction, the bearing area of the transverse ribs, and the vertical effective overburden stress all influence the bearing resistance at the transverse ribs. The passive bearing failure model (Figure 1) for geogrids in sandy soils is thus confirmed.

As described, the pullout behavior of the grid differs for sandy and clayey soils. It was discovered in this study that, under pullout action in clayey soils, a pullout failure plane was observed against the upper and lower surfaces of the longitudinal and transverse ribs of the grid. This is because the clay grains are very small and cohesive and also because the low angle of internal friction lessens shear resistance. This caused a "breakthrough" phenomenon that resulted from the knifelike cutting surface of the transverse ribs pressing against the soil in the grid's apertures during the pullout process. Figure 11 demonstrates that in clayey soils the bearing forces at the transverse ribs are not affected by confinement, and remain relatively stable. This explains why in clayey soils the passive resistance aspect of the pullout resistance is related to the degree of soil cohesiveness, and is not affected by confinement. Hence in the failure model depicted in Figure 1, there are no passive bearing zones; the only possibility is that failure is limited to elastic bearing zones. Thus, it can be seen that the formula of Jewell et al. (2) requires amendment, because it is not suitable for evaluating passive resis-

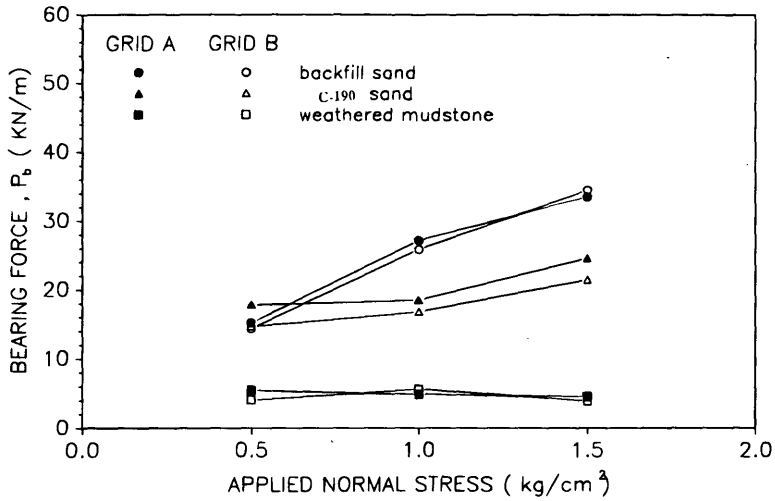

FIGURE 11 Comparison of bearing forces at the transverse ribs.

tance during pullout in cohesive soils. More data and further research are needed to establish the correct method.

Effect of Soil Confinement

Figure 9 shows the total pullout resistance of grids under normal stress in different soils. The pullout resistance of the grid increases with increasing confinement pressure, but the rate of increase differs depending on the soil type. Backfill sand gives higher rates of increase, and weathered mudstone gives the slowest rate of increase. Friction, the bearing capacity factors of soil passive resistance, and the angle of internal friction of the soil are all closely interrelated in terms of pullout resistance. Where the angle of internal friction of the soil is high, the bearing capacity factors will also be high, hence the relatively high rate of increase in pullout resistance as confinement pressure is increased for grids in sand backfill. By contrast, the rate of increase in pullout resistance as confinement pressure is increased is relatively low for grids in weathered mudstone. Furthermore, because the thickness of the grid is significant, when pullout forces are applied, the displacement results in dilation of soil particles, which leads to an increase in confined pressure. Hence pullout resistance tends to increase.

Strain Distribution Along Geogrid

Figures 12 and 13 are strain-distribution diagrams for all measurements of monitoring points at which the pullout displacement is 25 mm. The diagram clearly shows that when pulling forces are applied to the grid, the greatest strains are found at the measurement points nearest the portion where the pulling force is being applied,

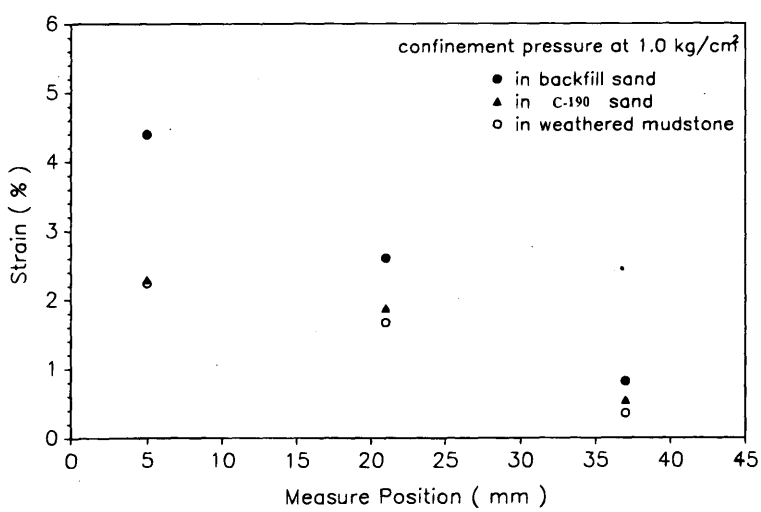

FIGURE 12 Strain distribution among all measuring points on Geogrid A when pullout displacement had reached 25 mm.

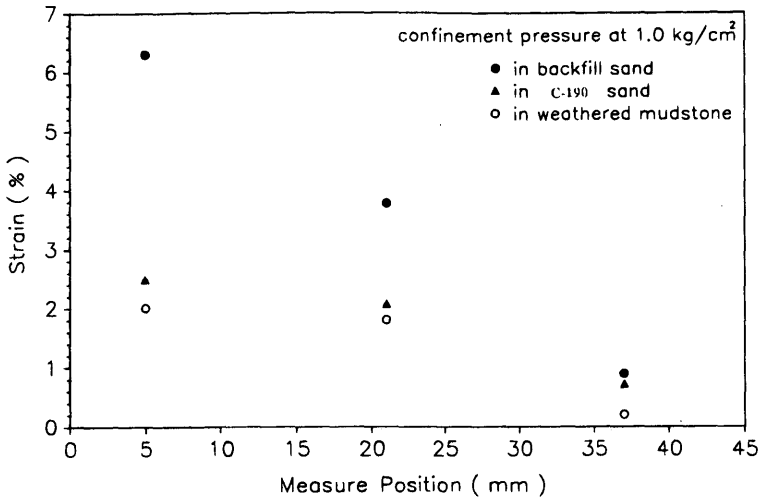

FIGURE 13 Strain distribution among all measuring points on Geogrid B when pullout displacement had reached 25 mm.

and most of the strain occurs at the two front measurement points. Thus most of the pullout resistance effect is provided by the grid's two front apertures. This unequal strain distribution under the pullout effect proves that strain transfer is uneven along the grid during pullout. This strain distribution pattern suggests that if the buried portion of the grid is too long strain will gradually be transferred from the front of the grid to the back when pulling forces are applied. This leads to the overdesign of the reinforcement material because when the front portion of the grid has achieved its maximum anchoring effect, the rear portion may not have undergone any deformation at all. This unequal strain-distribution phenomenon confirms the results obtained elsewhere (*6*).

CONCLUSION

Based on the foregoing, the following conclusions can be drawn from the analysis of the grid's mechanical characteristics.

- With the granular soil as the confining medium, soil passive resistance is the main contributor to the pullout resistance of the grid. With fine-grained soils as the confining medium, the proportion of pullout resistance composed of passive resistance decreased significantly.
- The pullout resistance of the grid increases as confining pressure increases. Where the angle of internal friction of the soil is high, the bearing capacity factors will also be high, so the grid exhibits a relatively faster rate of increase in pullout resistance as confining pressure is increased.
- For the grids used in the study, the pullout resistance in sandy soil was higher than in fine-grained soil.
- The strain distribution of the geogrid during testing was triangular; the strain gradually reduced from a maximum at the pullout end to zero at the other end.

REFERENCES

1. Bauer, G. E., and Y. M. Mowafy. The Effect of Grid Geometry and Aggregate Size on the Stress Transfer Mechanism. *Proc., 4th International Conference on Geotextiles, Geomembranes and Related Products*, Vol. 2, 1990, p. 801.
2. Jewell, R. A., G. W. E. Milligan, R. W. Sarsby, and D. Dubois. Interaction Between Soil and Geogrids. *Proc., Symposium on Polymer Grid Reinforcement in Civil Engineering*, Thomas Telford Limited, London, England, 1984, pp. 19–29.
3. Mitchell, J. K., and C. V. Villet. *NCHRP Report 290: Reinforcement of Earth Slopes and Embankments*. TRB, National Research Council, Washington, D.C., 1987.
4. Koerner, R. M. *GRI Test Methods and Standards: Geogrid Pullout*. Geosynthetic Research Institute, Drexel University, Philadelphia, Pa., 1992.
5. Wilson-Fahmy, R. F., R. M. Koerner, and L. J. Sansone. Experimental Behavior of Polymeric Geogrids in Pullout. *Journal of Geotechnical Division*, ASCE, Vol. 120, N. 4, 1994, pp. 661–677.
6. Holtz, R. D., and B. B. Broms. Wall Reinforced by Fabrics—Results of Model Test. *Proc., 1st International Conference on the Use of Fabrics in Geotecnics*, Paris, France, Vol. 1, 1977, pp. 113–117.

Publication of this paper sponsored by Committee on Geosynthetics.